Diffusion-Kinetic Modeling of the Electron Radiolysis of Water at Elevated Temperatures

Jay A. LaVerne* and Simon M. Pimblott

Radiation Laboratory, University of Notre Dame, Notre Dame, Indiana 46556

Received: October 22, 1992; In Final Form: January 5, 1993

The temperature dependence of the chemistry in the track of a fast electron in water has been examined with a deterministic diffusion–kinetic model. The model calculations suggest that there is an increase in the yields of the hydrated electron and hydroxyl radical and a decrease in the yields of molecular hydrogen and hydrogen peroxide with increasing temperature. These results are consistent with most of the experimental data. It is found that the best fit to the experimental data occurs when the radius of the initial spatial distribution of the hydrated electron is dependent on a process which scales according to an Arrhenius-like equation with an activation energy similar to that for electron movement between potential traps in water. The radii of the initial spatial distributions of all the other species appear to be independent of the temperature. The predictions of the model suggest that the initial radiation chemical yields of the reactive species are independent of temperature. An additional thermally dependent reaction for the decomposition of water is not required for the model predictions to match the experimental data.

Introduction

An obvious reason for understanding the radiation chemistry of water at elevated temperatures is the practical application of such knowledge to the design and maintenance of nuclear power reactors. However, such knowledge is also important for elucidating the basic processes which are responsible for the electron track structure at any temperature. Clearly, a diffusion–kinetic model which can predict the radiation chemical yields in water at various temperatures would be very useful in achieving these goals. There have been several attempts to model the steady-state radiation chemistry of water at temperatures up to 400 °C.[1-6] At a given temperature, these models assume a yield for the production of the radiation-induced reactive species in water, and they model the subsequent homogeneous chemistry. At present, there are a considerable number of inconsistencies in the literature as to the temperature dependences of the steady-state yields of the radiolytic products.[7]

The passage of a fast electron in liquid water produces a series of clusters of reactive species, called spurs. Within the spur, there is an initial nonhomogeneous spatial distribution of the reactive species.[8] It is the competition between diffusion into the bulk and intra-spur reactions which determines the steady-state yields of the reactive species, i.e., the yields remaining when the radiation-induced reactants become homogeneously distributed in the bulk medium. Both diffusion and reaction are known to be temperature dependent; however, it is not known which process will dominate the spur chemistry at high temperatures. In addition, the temperature dependences of the initial spur parameters are not known. It is possible that the initial spatial distributions of the reactive species are temperature dependent, and it has been postulated that there may be new thermally sensitive water decomposition processes.[2] All of these factors can have a large effect on the steady-state yield of the radiolytic products.

In this paper, the temperature dependence of the spur chemistry occurring in the fast electron radiolysis of water is examined. We have previously developed a deterministic diffusion–kinetic model based on a single "typical" spur which was parameterized to match the available experimental data on the production of hydrated electron, molecular hydrogen, hydroxyl radical, and hydrogen peroxide at 25 °C.[9] Furthermore, it has been shown that the predictions of this model agree well with those of a stochastic model for the radical species.[10] The following section of this paper describes in detail the parameters used in the diffusion–kinetic model including the temperature-dependent rate coefficients and diffusion coefficients. The third section contains a comparison of the model calculations with available experimental data and a discussion of the results. A summary of the work concludes.

Diffusion-Kinetic Model

The diffusion–kinetic calculations were performed using a numerical deterministic technique originally developed by Burns et al.[11] This technique was used in our previous studies and it is fully described there.[9,10] A single "typical" spur of 62.5 eV which represents the whole radiation chemical system is used. This spur is divided into concentric shells which are sufficiently narrow that the concentration of each of the species is homogeneous within each shell. The coupled differential equations describing the diffusion between adjacent shells and the reactions within the shells are solved with the FACSIMILE code which is based on the Gear algorithm.[12] The initial spatial distributions of the reactive species are assumed to be Gaussian. At 25 °C, the parameters of these distributions, the initial radiation chemical yields (G values in units of molecules/100 eV), the diffusion coefficients, and the rate coefficients are as used previously.[9]

In order to model the radiation chemistry of water at 25 °C, only 10 reactions are necessary.[13] These reactions and four more which must be included because of their high activation energies are given in Table I. It should be noted that fewer chemical reactions are necessary to describe the intra-spur chemistry of water than are needed to model the steady-state chemistry because of the different time scales involved. For instance, at 300 °C, the pH of pure water is near 5,[14] and various ionic reactions between the radiation-induced species and the bulk ions are possible. However, these reactions predominantly occur after 1 μs and intra-spur processes are complete. The same arguments can be applied to the known thermal decomposition of hydrogen peroxide at high temperatures.[3]

The rate coefficients listed in Table I are the values at 25 °C.[15] Temperature scaling of these coefficients from the 25 °C values was performed in a variety of different ways based on the available experimental data. The temperature dependences of those rate coefficients in Table I that are listed as being scaled tabularly were taken directly from tables or figures of ref 16 or 17 and were normalized to the 25 °C values of ref 15. Several rate coefficients were scaled using an Arrhenius equation, and they are listed with the appropriate activation energy, E_a.[18-25] No satisfactory

0022-3654/93/2097-3291$04.00/0

TABLE I: Reactions Included in the Diffusion-Kinetic Modeling of Water

	reaction		k at 25 °C,[15] M^{-1} s^{-1}	temp scaling[a]	ref
		Water Reactions			
R1	$e^-_{aq} + e^-_{aq}$	$\rightarrow H_2 + OH^- + OH^-$	5.5×10^9	tabular	16
R2	$e^-_{aq} + H^+$	$\rightarrow H$	2.3×10^{10}	tabular	17
R3	$e^-_{aq} + H$	$\rightarrow H_2 + OH^-$	2.5×10^{10}	diffusion	
R4	$e^-_{aq} + OH$	$\rightarrow OH^-$	3.0×10^{10}	diffusion	
R5	$e^-_{aq} + H_2O_2$	$\rightarrow OH + OH^-$	1.1×10^{10}	tabular	17
R6	$H^+ + OH^-$	$\rightarrow H_2O$	1.4×10^{11}	Arrhenius, E_a = 10.5	18
R7	$H + H$	$\rightarrow H_2$	7.8×10^9	Arrhenius, E_a = 14.7	19
R8	$H + OH$	$\rightarrow H_2O$	2.0×10^{10}	Arrhenius, E_a = 7.87	20
R9	$H + H_2O_2$	$\rightarrow H_2O + OH$	9.0×10^7	Arrhenius, E_a = 16.4	21
R10	$OH + OH$	$\rightarrow H_2O_2$	5.5×10^9	tabular	17
R11	$H + OH^-$	$\rightarrow H_2O + e^-_{aq}$	1.8×10^7	Arrhenius, E_a = 38.5	22
R12	$OH + H_2$	$\rightarrow H + H_2O$	4.0×10^7	Arrhenius, E_a = 19.0	23
R13	$OH + H_2O_2$	$\rightarrow HO_2 + H_2O$	3.0×10^7	Arrhenius, E_a = 14.0	24
R14	$HO_2 + HO_2$	$\rightarrow H_2O_2 + O_2$	8.0×10^5	Arrhenius, E_a = 20.6	25
		Oxygen Reactions			
R15	$e^-_{aq} + O_2$	$\rightarrow O_2^-$	1.9×10^{10}	tabular	17
R16	$H + O_2$	$\rightarrow HO_2$	2.1×10^{10}	tabular	17
R17	$H^+ + O_2^-$	$\rightarrow HO_2$	3.8×10^{10}	Arrhenius, E_a = 10.5	18
		Ferrous Ion Reactions			
R18	$Fe^{2+} + H$	$\rightarrow Fe^{3+} + H_2 + OH-$	7.5×10^6	Arrhenius, E_a = 12.6	3
R19	$Fe^{2+} + OH$	$\rightarrow Fe^{3+} + H_2O + OH^-$	4.3×10^8	Arrhenius, E_a = 9.2	3
R20	$Fe^{2+} + H_2O_2$	$\rightarrow Fe^{3+} + OH + H_2O + OH^-$	4.2×10^1	Arrhenius, E_a = 41.9	3
R21	$Fe^{2+} + HO_2$	$\rightarrow Fe^{3+} + H_2O_2 + OH^-$	2.1×10^6	Arrhenius, E_a = 41.9	3
R22	$Fe^{3+} + H$	$\rightarrow Fe^{2+} + H^+$	2.0×10^6	Arrhenius, E_a = 12.6	3

[a] E_a values in kJ/mol.

experimental data were found for the temperature dependences of reactions R3 and R4. Previous model calculations scaled these two reactions using an Arrhenius equation with an activation energy of 12.6 kJ/mol.[2] However, Elliot et al.[17] have pointed out that, for a number of reasons, the values obtained are not very accurate. Except where otherwise noted, the rate coefficients for reactions 3 and 4 were scaled according the self-diffusion in water. Such scaling is thought to be sufficient because these reactions have large rate coefficients at 25 °C and they are believed to be close to diffusion-controlled. Some trial calculations were performed in which the rate coefficients of reactions R3 and R4 were scaled using an Arrhenius equation with an activation energy of 12.6 kJ/mol. The differences observed in the results are discussed in the following section. Scaling of the rate coefficients for the ferrous ion reactions was performed either with the Arrhenius parameters given in Table I or in some cases by the self-diffusion in water. Figure 1 shows the rate coefficients for reactions R1–R14 as a function of temperature. It is clearly seen in this figure that a simple Arrhenius scaling of all the rate coefficients can give values that are significantly different from those determined experimentally.

A complete assessment of the self-diffusion in liquid water was performed by Weingartner.[26] He suggested that the temperature-dependent studies of Krynicki et al.[27] were the most reliable. These later authors found that a good representation of their experimental data could be obtained from the following equation,

$$D(H_2O) = 12.5 \times 10^{-9} T^{1/2} \exp(-925/(T - 95))$$

where D has the units of m^2 s^{-1} and T is in kelvin. This equation for the self-diffusion in water was used to scale the diffusion coefficients of the hydrated electron, hydrogen atom, molecular hydrogen, hydroxyl radical, and hydrogen peroxide and a number of rate coefficients, as noted above, from their values at 25 °C. There are no experimental data available on the temperature dependences of these diffusion coefficients except for the hydrated electron which was found to agree well with a scaling of the 25 °C value according to the self-diffusion in water.[28] The diffusion coefficients for the proton and hydroxide ion were taken from compilations of experimental data.[29,30] The temperature dependences of the diffusion coefficients used are shown in Figure 2.

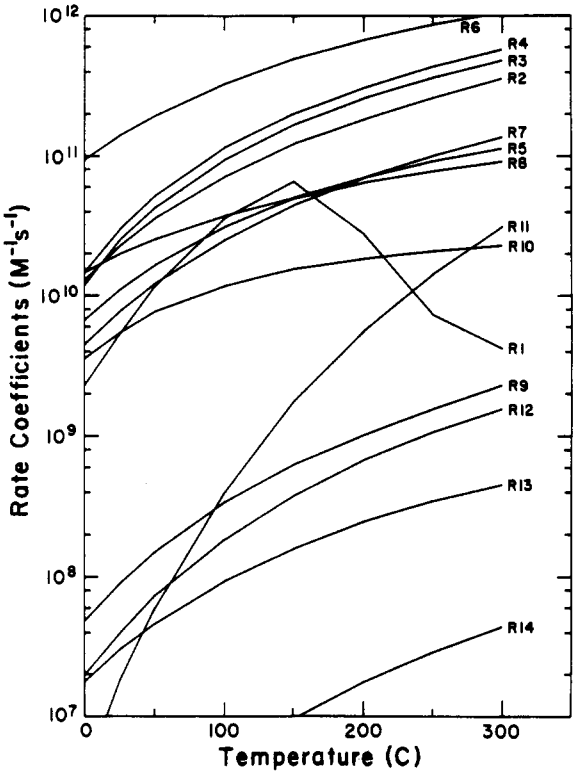

Figure 1. Variation of the rate coefficients for the reactions listed in Table I as a function of temperature. The method used for the temperature scaling for each reaction rate coefficient is given in Table I.

The temperature dependences of the radii representative of the initial spatial distributions of the reactive species in the spur are completely unknown. It is usually assumed, as was done in this work, that the initial distributions of the reactive species are Gaussian, but the exact mechanisms responsible for these distributions are not well understood. Model calculations were performed using a variety of assumptions for the temperature dependences of the radii for the initial spatial distributions. Previous work[9] has shown that the best fit of the predictions of the diffusion–kinetic model to the experimental data at 25 °C is obtained when the radius (standard deviation) of the hydrated

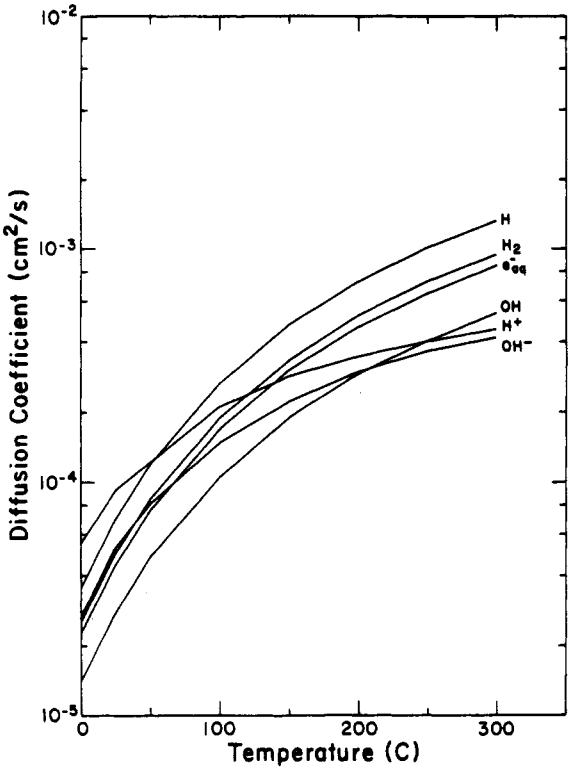

Figure 2. Variation of the diffusion coefficients for the reactive species as a function of temperature. Experimental data are used for H^+ [29] and OH^-,[30] and all other coefficients are scaled to the self-diffusion in water.[31]

electron distribution is taken to be 2.3 nm and all other species have distributions with radii of 0.85 nm. In some of the diffusion–kinetic calculations reported, one or both of these radii were assumed to be independent of temperature. In other calculations, the radii of the distributions were assumed to scale according to the self-diffusion in water. For several calculations, an activation energy of 9.6 kJ/mol was used to scale the radius of the hydrated electron spatial distribution using an Arrhenius-like equation. This activation energy corresponds to that suggested by Cercek[31] for the movement of the hydrated electron between potential traps in water.

Results and Discussion

Since very little is known about the processes responsible for the structure of a spur produced by a fast electron, the model calculations were performed using a number of assumptions for the temperature dependences of the initial spatial distributions of the reactive species. The results of the diffusion–kinetic calculations for pure water at 1 μs using various radii are compared with selected data of Elliot et al.[32] on Figure 3 for the reducing species (hydrated electron, hydrogen atom, and molecular hydrogen). Similar comparisons for the oxidizing species (hydroxyl radical and hydrogen peroxide) are shown in Figure 4. For a type 1 spur where the initial spur radii are kept constant at the 25 °C values (2.3 nm for the hydrated electron, 0.85 nm for the rest), the modeled radical yields are much less than those observed experimentally. At high temperatures, there is an increase in intra-spur reactions over diffusion, so fewer radicals exist at 1 μs to escape the spur. On the other hand, for a type 2 spur where both radii are temperature scaled according to the self-diffusion in water, the predicted radical yields are considerably greater than the experimental data. In this limit at high concentrations, scaling the radii according to the self-diffusion in water results in a large spur, and consequently, the initial concentrations of the reactive species are so diffuse that virtually no chemical reactions occur before the reactants escape into the bulk. At 300 °C, the radius of the hydrated electron is 10.0 nm, while the other radii are 3.7 nm.

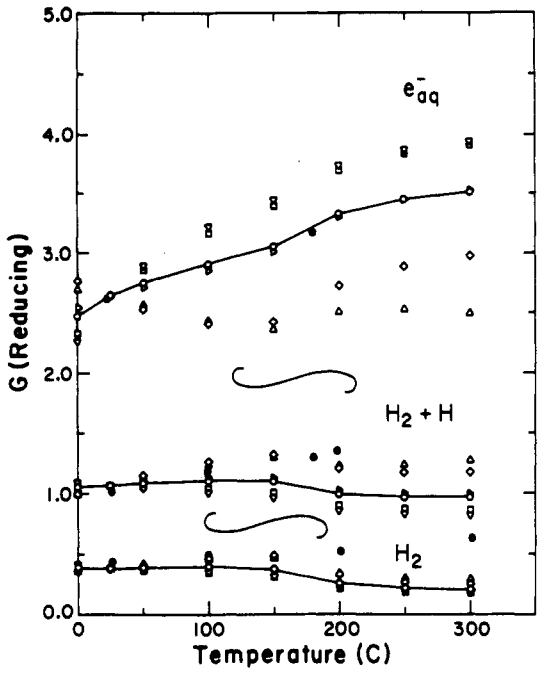

Figure 3. Variation of the radiation chemical yields of the reducing species with temperature for different temperature dependences of the initial spur radii. Experimental data (●) are from ref 32, and the results of the model calculations are as follows: (△) type 1, $R_{e^-_{aq}}$ = constant, R_{H^+} = constant; (□) type 2, $R_{e^-_{aq}} \propto$ self-diffusion in water, $R_{H^+} \propto$ self-diffusion in water; (◇) type 3, $R_{e^-_{aq}}$ = constant, $R_{H^+} \propto$ self-diffusion in water; (▽) type 4, $R_{e^-_{aq}} \propto$ self-diffusion in water, R_{H^+} = constant; (○) type 5, $R_{e^-_{aq}}$ activation controlled, R_{H^+} = constant; and (▷) type 6, $R_{e^-_{aq}}$ activation controlled, $R_{H^+} \propto$ self-diffusion in water. The radii of all the species except the hydrated electron are the same as for H^+.

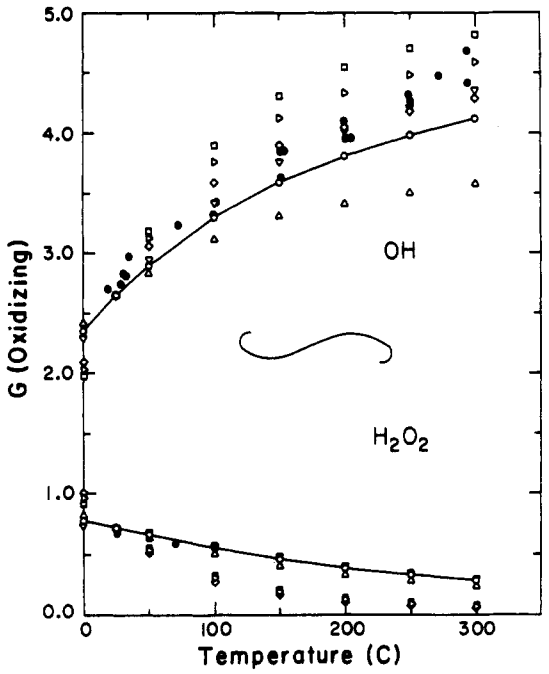

Figure 4. Variation of the radiation chemical yields of the oxidizing species with temperature for different temperature dependences of the initial spur radii. Symbols are the same as in Figure 3.

Calculations were also performed in which one of the radii was held constant while the other was varied according to the temperature dependence of self-diffusion in water, types 3 and 4 spurs. A correlation exists between the distributions for the hydrated electron and the hydroxyl radical and the predicted steady-state yields. The hydrated electron and the hydroxyl radical react mainly with each other in the spur so that any factor that affects the yield of one species also influences the other. It

is found that if the hydrated electron radius is constant with temperature and the radii of the other reactants vary according to the self-diffusion in water, the yield of the hydroxyl radical is greater than if all radii are constant. The same result is found if the temperature dependences of the radii are reversed. Either situation gives reasonably good agreement between the model and experimental data for the hydroxyl radical, but the yield of the hydrated electron is too large or too small when compared to the experimental data. These calculations show that at high temperatures, the yields of the hydrated electron and molecular hydrogen are determined to a large extent only by the radius of the initial spatial distribution of the hydrated electron. The yields of the oxidizing species are not very dependent on this radius as long as it is not constant with temperature.

Scaling the radius of the initial distribution of the hydrated electron according to the self-diffusion in water always overestimates the hydrated electron yield in the model calculations so that the true value must be somewhat less than predicted in this manner. The temperature dependence of the initial distribution of the hydrated electron is determined by the distance the secondary electron travels until it is solvated. Calculations on the energy deposition of fast electrons in water suggest that the average energy loss in a spur is about 40 eV.[33] Virtually all of the energy deposited in the spur in excess of the ionization potential of water goes into the kinetic energy of a secondary electron which itself may ionize other water molecules to produce more electrons. Electrons with energy greater than the ionization potential of water lose energy through Coulombic interactions with the bound electrons of water, and these processes are more-or-less independent of temperature. However, the energy loss processes of electrons with energies less than the subexcitation energy of water, and the solvation process itself, may well be strongly temperature dependent. Therefore, it was assumed that these processes could be approximated by the movement of the electron between potential traps in water. Cercek[31] estimated that the activation energy for such movement is 9.6 kJ/mol. An Arrhenius-like scaling of the radius for the spatial distribution of the hydrated electron gives a value of 5.8 nm at 300 °C.

At high temperatures, the diffusion–kinetic calculations give results which accurately match the experimental data when the other radii are held constant or they are varied according to the self-diffusion in water. However, at the lower temperatures, the best fit of the data for both the hydrated electron and hydroxyl radical yields is obtained when the radius of the initial spatial distribution of the hydrated electron is determined by an Arrhenius-like scaling and the other radii are kept constant, a type 5 spur. The production of secondary electrons by the initial energy loss event and many of the subsequent events within the spur lead to the formation of cations which are the source of most of the reactive species formed.[8] These energy loss events result from interactions of electrons which are relatively energetic, and they are due to Coulombic interactions which are not dependent on temperature. Consequently, all of the reactive species, except hydrated electrons, are formed initially near the center of the spur in processes which are not temperature dependent. Excitation of water followed by its dissociation may also occur, but these excitation processes must occur near the center of the spur before the secondary electrons have lost too much energy. The diffusion–kinetic calculations presented suggest that for all of the reactive species except the hydrated electrons, there is little dependence on temperature of the processes leading to their formation.

The predictions of the diffusion–kinetic model for the temperature dependence of the yield of hydrated electron in a type 5 spur are shown in Figure 5 and are compared with all of the available experimental data.[32,34] Figure 5 also contains the diffusion–kinetic predictions for the yield of molecular hydrogen and the corresponding experimental data.[32,35-38] For the most part, agreement between the model calculations and the experimental data is good, although there is a considerable amount of scatter in some of the experimental data. The major disagreement between the model calculations and experiment is for the molecular hydrogen yield at high temperatures. The model predicts a slight decrease in the molecular hydrogen yields with increasing temperature, while the experimental data seem to remain constant. We do not regard this difference as significant considering the large discrepancy between the different sets of experimental data. Past experience with model calculations suggests that the deterministic diffusion–kinetic model works better for predicting radical yields than molecular yields.[10] The use of a stochastic model would probably give better results for the molecular yields. The H atom yields are not shown in Figure 5 because of the large uncertainties in their yields. They are determined from the differences in the yields for molecular hydrogen observed in systems with and without H atom scavengers. The diffusion–kinetic model suggests that the H atom yield increases by less than 0.1 molecule/100 eV from 25 to 300 °C.

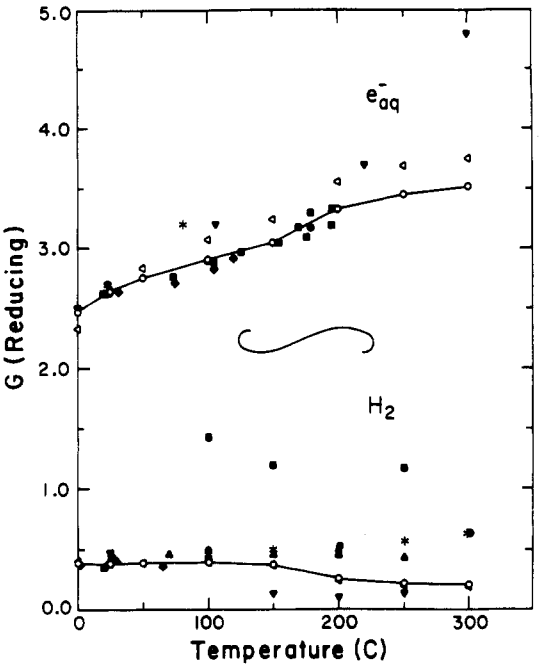

Figure 5. Radiation chemical yields of the reducing species as a function of temperature. The diffusion–kinetic predictions are given by the ○ symbols and the solid line. The experimental points for the hydrated electron are ●, ■, and ◆ (ref 32) and ▼ and ✱ (ref 34), and those for molecular hydrogen are ● (ref 32), ■ (ref 35), ● (ref 36), ▲ (ref 37), and ▼ and ✱ (ref 38). Model calculations with activation-energy-controlled rate coefficients for reactions 3 and 4 are given by ◁.

The results of diffusion calculations for the temperature dependence of the yields of the oxidizing species are shown in Figure 6 and are compared with the experimental data for the hydroxyl radical[32,35,36] and for hydrogen peroxide.[32,35,36] The model predictions are slightly lower than the experimental data for hydroxyl radicals especially above 200 °C. One of the reasons for this discrepancy is because the model was used to predict the yield of hydroxyl radicals in deaerated water, whereas the chemical systems all contain oxygen. The use of oxygen or other scavengers to remove the hydrated electron increases the scavengable yield of the hydroxy radical. This cooperative effect has been studied extensively for the hydroxy radical, and it can be quite substantial.[39] A set of diffusion–kinetic calculations were made for water with a constant oxygen concentration of 1.25 mM. The results are in excellent agreement with the experimental data as shown in Figure 6.

Experimental measurements of the hydroxyl radical yield are difficult at any temperature. They are generally made using systems that are chemically unstable at high temperature. Model calculations and experiments are both susceptible to large

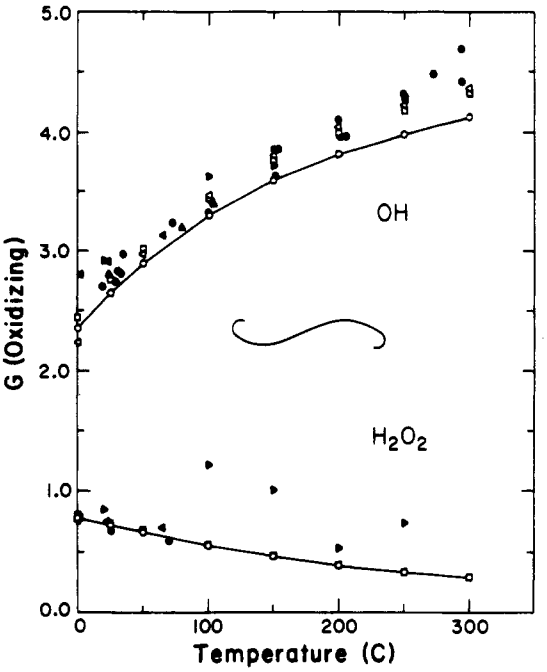

Figure 6. Radiation chemical yields of the oxidizing species as a function of temperature. The diffusion–kinetic predictions are given by the ○ symbols and the solid line. The experimental points for the hydroxyl radical are ▲ and ● (ref 32), ▶ (ref 35), and ◀ (ref 36), and those for hydrogen peroxide are ● (ref 32), ▶ (ref 35), and ◀ (ref 36). Model calculations with activation-controlled rate coefficients for reactions 3 and 4 are given by ◁. Model calculations for 1.25 mM oxygen solution are given by □.

uncertainties. Two of the reactions, reactions R3 and R4 in the reaction scheme listed in Table I, do not have reliable data for the temperature dependence of their rate coefficients. Burns and Marsh[2] considered these reactions to be activation energy controlled with an E_a of 12.6 kJ/mol. Elliot[21] has argued that the indiscriminate use of this activation energy is inappropriate. Nevertheless, calculations were performed on deaerated water with such an activation-energy-controlled rate for reactions R3 and R4, and the results are included in Figures 5 and 6. At 300 °C the activation-energy-scaled rate coefficients of reactions R3 and R4 are 60% of those obtained by scaling to the self-diffusion in water. There is no observable effect on the molecular hydrogen and hydrogen peroxide yields while the hydrated electron and hydroxyl radical yields are increased.

Burns and Marsh[2] suggested that an additional source of water decomposition might become significant at high temperatures. They postulated that water decomposed to give molecular hydrogen and the oxygen atom. The predominant oxygen atom reaction is with water to give two hydroxyl radicals. At 300 °C, the diffusion–kinetic model predicts a yield of molecular hydrogen which is about 0.4 molecule/100 eV smaller than experimentally measured by Elliot et al.[32] If an additional water decomposition mechanism, as proposed by Burns and Marsh, were responsible for this difference, then 0.8 molecule/100 eV of hydroxyl radicals would also be produced. Such a large additional production of hydroxyl radicals is not observed. Obviously, better data and especially better rate coefficients for reactions R3 and R4 are necessary to fully resolve the question. Based on the present calculations, it appears that if there is any additional thermal decomposition of water, it must be relatively small and occur only at temperatures above 200 °C.

The relative temporal variation of the yield of the hydrated electron has been measured at elevated temperatures,[16,40,41] but no one has published absolute yields. Figure 7 contains the results of diffusion–kinetic calculations for the time-dependent yield of the hydrated electron in type 1, 2, and 5 spurs. Changing the radii from being independent of temperature, type 1, to having

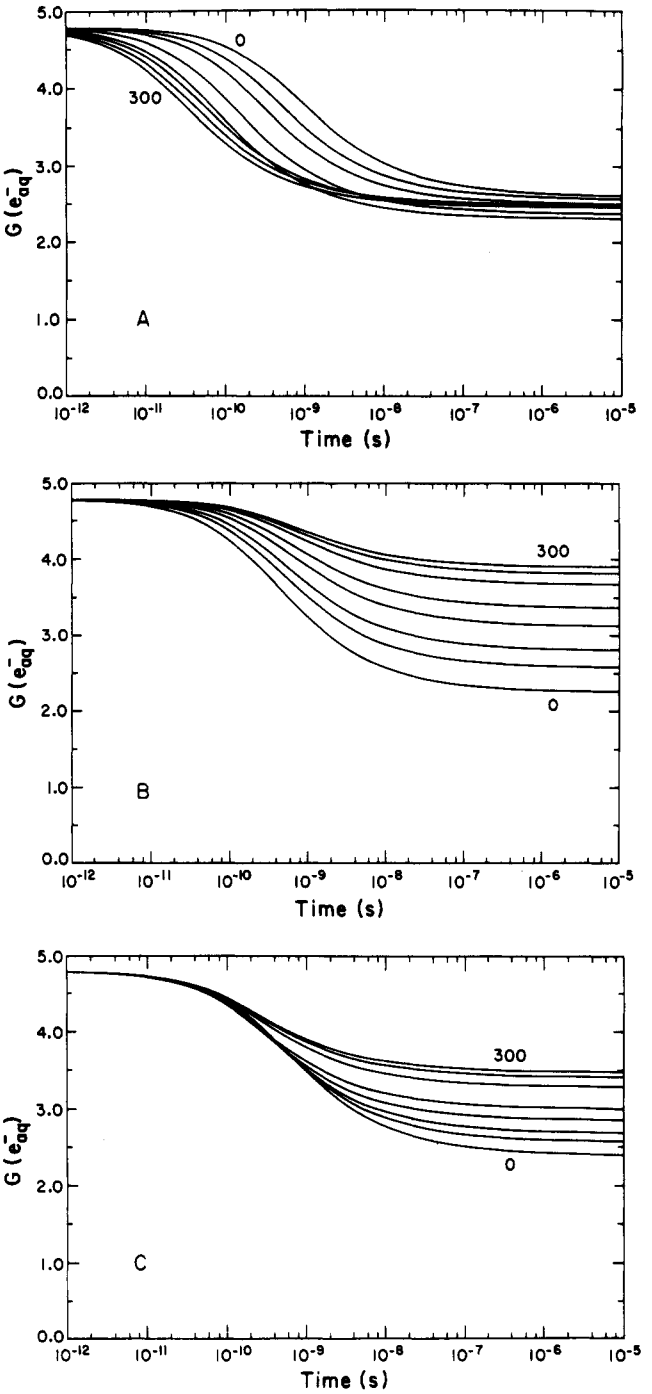

Figure 7. Temporal variation of the hydrated electron at 0, 25, 50, 100, 150, 200, 250, and 300 °C. The various assumptions for the temperature dependence of initial radii are as follows: (a) type 1, $R_{e^-_{aq}}$ = constant, R_{H^+} = constant; (b) type 2, $R_{e^-_{aq}} \propto$ self-diffusion in water, $R_{H^+} \propto$ self-diffusion in water; and (c) type 5, $R_{e^-_{aq}}$ activation controlled, R_{H^+} = constant. The radii of all the species except the hydrated electron are the same as for H^+.

the same temperature dependence as the self-diffusion in water, type 2, completely reverses the relative temperature dependence of the yields at subnanosecond times. The three different spur types give very different temporal dependences. The results of the scavenging experiments of Shiraishi et al.[41] suggest that less intra-spur reaction of the hydrated electron occurs at higher temperatures. The time profile data measured are consistent with this conclusion in that they show less hydrated electron decay over the time period of a few nanoseconds to about 400 ns as the temperature increases. The decays for type 5 spurs in Figure 7 show this same trend. The type 1 spur gives the opposite results. It is clear that the radius of the initial distribution of the hydrated electron must increase with increasing temperature.

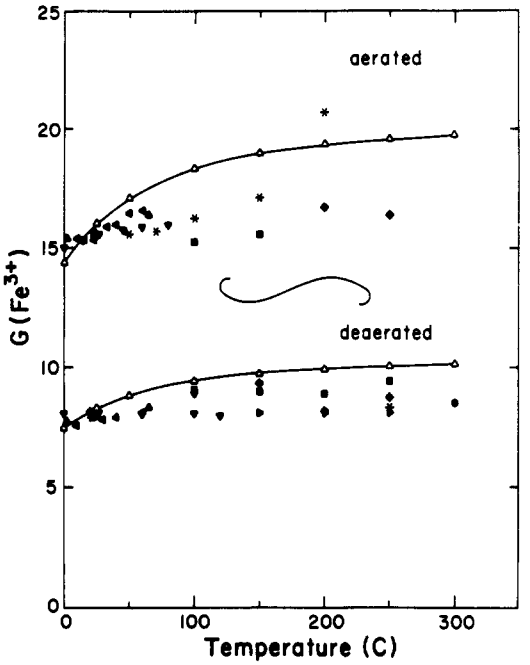

Figure 8. Radiation chemical yield of the ferric ion in the radiolysis of the aerated and deaerated Fricke dosimeter as a function of temperature. The diffusion-kinetic predictions are given by the △ symbol. The experimental data are ◆ (ref 3), ● (ref 7), ■ (ref 35), ▲ (ref 36), ✱ (ref 42), ▼ (ref 44), ▶ (ref 45), and ◀ (ref 46).

One of the most common aqueous systems studied at elevated temperatures is the oxidation of ferrous ions in the Fricke dosimeter. Figure 7 contains the results of diffusion-kinetic calculations and the experimental data[3,7,35,36,42-46] for this system. It is generally accepted that the ferric ion yields in aerated and deaerated solutions have a small temperature dependence. The results of the diffusion-kinetic model are 20% and 15% greater than the experimental results for aerated and deaerated solutions, respectively, at 250 °C. The reason for the discrepancy is unknown. The temperature dependences of the rate coefficients used for the ferrous reactions listed in Table I are not well-known. However, there is only a very minor dependence of the ferric ion yield on these rate coefficients since most of the chemistry in a 1 mM solution occurs after the nonhomogeneous spur reaction is completed. The time dependence of the ferric ion yield will change, but not the total end point. This conclusion was checked with the diffusion-kinetic model using rate coefficients which were scaled to the self-diffusion in water. Differences in the total ferric ion yield of less than 0.1% were found. Such differences are too small to account for the discrepancy with experimental data. It has been suggested that hydrogen peroxide decays at high temperatures;[3] however, the product of this decay is two hydroxyl radicals, so there is no net change in the yield of the ferrous oxidation. Another source of error in the model is the reduction of ferric ions to ferrous. The only reaction included in the present reaction scheme is the hydrogen atom reduction, reaction R22, which is found to have no significant effect on the ferric ion yield. The diffusion-kinetic model uses the ferrous ion reactions listed in Table I. It is assumed that the anions associated with the iron cations do not effect the total ferric ion yield observed. However, the experiments measure the steady-state yield of stable complexes of the ferric ion with sulfate which absorb at 304 nm.[47] The dissociation of these complexes at high temperatures is not taken into account in the diffusion-kinetic model but is implicit in the experiment. Clearly the results of the calculations in Figure 8 represent an overestimation of the observed ferric ion yield. There is some indication that there is an experimental problem leading to the apparent independence of the ferric ion yields with temperature. Those experimental studies in which the Fricke dosimeter was used in conjunction with other systems to estimate the radiolytic yields generally give results which do not agree with other data available (see, for instance, the data of Katsumura et al.[35] on Figures 5 and 6). More investigations of this system have to be performed experimentally and with kinetic models.

Summary

The temperature dependence of the kinetics in the track of a fast electron in water has been examined with a deterministic diffusion-kinetic model. The model calculations suggest an increase in the yields of the hydrated electron and the hydroxyl radical and a decrease in molecular hydrogen and hydrogen peroxide with increasing temperature. These results are consistent with most of the available experimental data. It is found that the initial spur radius of the hydrated electron is dependent on a process which has an activation energy similar to that found for the movement of the hydrated electron between potential traps in water while the radii of all the other species are independent of the temperature. The model also suggests that the initial radiation chemical yields of the reactive species are independent of temperature, and it does not require an additional thermally dependent reaction for the decomposition of water.

Acknowledgment. The work described herein was supported by the Office of Basic Energy Sciences of the Department of Energy. This is Contribution NDRL-3544 of the Notre Dame Radiation Laboratory. We thank Dr. A. J. Elliot and Dr. G. V. Buxton for providing their experimental data prior to publication.

References and Notes

(1) Burns, W. G.; Moore, P. B. *Radiat. Eff.* **1976**, *30*, 233.
(2) Burns, W. G.; Marsh, W. R. *J. Chem. Soc., Faraday Trans. 1* **1981**, *77*, 197.
(3) Takagi, J.; Ishigure, K. *Nucl. Sci. Eng.* **1985**, *89*, 177.
(4) Ibe, E.; Uchida, S. *Nucl. Sci. Eng.* **1985**, *90*, 140.
(5) Ishigure, K.; Takagi, J.; Shiraishi, H. *Radiat. Phys. Chem.* **1987**, *29*, 195.
(6) Lukac, S. R. *Radiat. Phys. Chem.* **1989**, *33*, 223. For further comments on this paper, see also: Elliot, A. J. *Radiat. Phys. Chem.* **1990**, *36*, 863. Lukac, S. R. *Radiat. Phys. Chem.* **1990**, *36*, 865.
(7) Elliot, A. J.; Ouellette, D. C.; Reid, D.; McCracken, D. R. *Radiat. Phys. Chem.* **1989**, *34*, 747.
(8) Farhataziz; Rodgers, M. A. J., Eds. *Radiation Chemistry. Principles and Applications*; VCH Publishers: New York, 1987.
(9) LaVerne, J. A.; Pimblott, S. M. *J. Phys. Chem.* **1991**, *95*, 3196.
(10) Pimblott, S. M.; LaVerne, J. A. *Radiat. Res.* **1990**, *122*, 12.
(11) Burns, W. G.; Sims, H. E.; Goodall, J. A. B. *Radiat. Phys. Chem.* **1984**, *23*, 143-180.
(12) Chance, E. M.; Curtis, A. R.; Jones, I. P.; Kirby, C. P. Report AERE-R 8775, AERE, Harwell, 1977.
(13) Schwarz, H. A. *J. Phys. Chem.* **1969**, *73*, 1928.
(14) Marshall, W. L.; Frank, E. U. *J. Phys. Chem. Ref. Data* **1981**, *10*, 295.
(15) Buxton, G. V.; Greenstock, C. L.; Helman, W. P.; Ross, A. B. *J. Phys. Chem. Ref. Data* **1988**, *17*, 513.
(16) Christensen, H.; Sehested, K. *J. Phys. Chem.* **1986**, *90*, 186.
(17) Elliot, A. J.; McCracken, D. R.; Buxton, G. V.; Wood, N. D. *J. Chem. Soc., Faraday Trans.* **1990**, *86*, 1539.
(18) Eigen, M.; de Maeyer, L. *Naturwissenschaften* **1955**, *42*, 413. This reference gives a range of activation energies of 8.5-12.5 kJ mol^{-1}, and an average was taken. The average value is equal to that measured by Barker et al.[28] but somewhat smaller than that obtained more recently by Natzle and Moore: Natzle, W. C.; Moore, C. B. *J. Phys. Chem.* **1985**, *89*, 2605.
(19) Sehested, K.; Christensen, H. *Radiat. Phys. Chem.* **1990**, *36*, 499.
(20) Buxton, G. V. Private communication.
(21) Elliot, A. J. *Radiat. Phys. Chem.* **1989**, *34*, 753.
(22) Han, P.; Bartels, D. M. *J. Phys. Chem.* **1990**, *94*, 7294.
(23) Christensen, H.; Sehested, K. *J. Phys. Chem.* **1983**, *87*, 118.
(24) Christensen, H.; Sehested, K.; Corfitzen, H. *J. Phys. Chem.* **1982**, *86*, 1588.
(25) Christensen, H.; Sehested, K. *J. Phys. Chem.* **1988**, *92*, 3007.
(26) Weingartner, H. *Z. Phys. Chem. N. F.* **1982**, *132*, 129.
(27) Krynicki, K.; Green, C. D.; Sawyer, D. W. *Discuss. Faraday Soc.* **1978**, *66*, 199.
(28) Barker, G. C.; Fowles, P.; Sammon, D. C.; Stringer, B. *J. Chem. Soc., Faraday Trans. 1* **1970**, *66*, 1498.
(29) Miller, D. G. *Lawrence Livermore National Laboratory Report 53319*, 1982.
(30) Quist, A. S.; Marshall, W. L. *J. Phys. Chem.* **1965**, *69*, 2984.
(31) Cercek, B. *J. Phys. Chem.* **1968**, *72*, 2279.

(32) Elliot, A. J.; Chenier, M. P.; Ouellette, D. C. Submitted to *J. Chem. Soc., Faraday Trans.*
(33) Pimblott, S. M.; LaVerne, J. A.; Mozumder, A.; Green, N. J. B. *J. Phys. Chem.* **1990**, *94*, 488.
(34) Jha, K. N.; Ryan, T. G.; Freeman, G. R. *J. Phys. Chem.* **1975**, *79*, 868.
(35) Katsumura, Y.; Takeuchi, Y.; Ishigure, K. *Radiat. Phys. Chem.* **1988**, *32*, 259.
(36) Hochanadel, C. J.; Ghormley, J. A. *Radiat. Res.* **1962**, *16*, 653.
(37) Kabakchi, S. A.; Lebedeva, I. E. *High Ener. Chem.* **1982**, *16*, 248.
(38) Elliot, A. J.; Chenier, M. P.; Ouellette, D. C. *Can. J. Chem.* **1990**, *68*, 712.
(39) LaVerne, J. A.; Pimblott, S. M. Submitted to *J. Chem. Soc., Faraday Trans.*
(40) Shiraishi, H.; Katsumura, Y.; Hiroishi, D.; Ishigure, K.; Washio, M. *J. Phys. Chem.* **1988**, *92*, 3011.
(41) Shiraishi, H.; Katsumura, Y.; Ishigure, K. *Radiat. Phys. Chem.* **1989**, *34*, 705.
(42) Kabakchi, S. A.; Lebedeva, I. E. *High Ener. Chem.* **1984**, *18*, 166.
(43) Kabakchi, S. A.; Lebedeva, I. E. *High Ener. Chem.* **1986**, *20*, 307.
(44) Balakrishnan, I.; Reddy, M. P. *J. Phys. Chem.* **1972**, *76*, 1273.
(45) Kubota, H. *J. Inorg. Nucl. Chem.* **1966**, *28*, 3053.
(46) Matthews, R. W. *Int. J. Appl. Radiat. Isot.* **1982**, *33*, 1159.
(47) Jayson, G. G.; Parsons, B. J.; Swallow, A. J. *Int. J. Radiat. Phys. Chem.* **1975**, *7*, 363.